Rev. Roum. Sci. Techn.– Électrotechn. et Énerg.
Vol. **67**, *2*, pp. 145–150, Bucarest, 2022

A NOVEL DC-DC CONVERTER FED BY PV SOURCE EMPLOYING IMPROVED INCREMENTAL CONDUCTANCE ALGORITHM UNDER PARTIAL SHADOW CONDITIONS

RAKESH THANKAKAN[1], EDWARD RAJAN SAMUEL NADAR[2*]

Keywords: Photovoltaic system; High gain dc-dc converter; Maximum power point tracking; Improved incremental conductance algorithm.

Photovoltaic (PV) self-consumption is essential for storing and deferring energy generated from distributed solar energy systems. This paper investigates a novel high-gain dc-dc converter for extraction of maximum power from the solar PV system by employing both incremental conductance (I&C) and improved incremental conductance (IIC) based on maximum power point tracking (MPPT) techniques under partial shadow conditions. This proposed converter achieves high step-up voltage gain using voltage doublers and improves the system's efficiency with low voltage stress on the switch, reduced reverse recovery of diodes, and less duty cycle operation. It avoids the converter operation at extreme duty cycles. The simulation responses to the work have been simulated using a MATLAB-Simulink environment, and the obtained results are validated through an experimental prototype.

1. INTRODUCTION

The use of green power diminishes the dependency on fossil fuels used and the amount of CO_2 released into the atmosphere. One of the most user-friendly alternative green resources is the solar PV system used in many residential, agricultural, transportation, and industrial sectors. Since a PV cell is a low-power device, stacks of PV cells give the output voltage in the range of 24 V to 40 V, depending on the manufacture of PV technologies. Further, these voltage ranges are boosted to the required level using a dc-dc power converter and MPPT controller circuits. Figure 1 illustrates a graphic illustration of the planned work. A conventional boost converter [1–3] provides high voltage gain with a significant duty ratio. The system's conversion efficiency and step-up voltage gain are reduced due to equivalent series resistance of inductors and capacitors, losses of power switches and diodes, and the reverse-recovery issues of diodes. The voltage lift technique does not perform better due to the high transient current at the switches and more conduction losses [4,5]. Even though voltage multiplier cells (VMCs) [6] reduce the conversion efficiency and give the steady-state voltage gain, it requires more circuit components. The phase-shifted full-bridge transformer [7] increases the transformer's turn ratio to achieve the required high voltage gain. On the other hand, the output-diode voltage stress is significantly larger than the output voltage, forcing the use of input electrolytic capacitors to mitigate the excessive input current ripple. A high step-up dc-dc converter with integrated coupled inductor and voltage multiplier circuits achieves high step-up voltage gain [8], with obtained efficiency of 93.5 %. The analysis of magnetically coupled dc-dc converter [9] for integrating renewable energy systems in smart grid applications was discussed. It investigated the effect of the magnetic coupling coefficient (k) on improving the performance of boost dc-dc converters for renewable energy systems. Since a PV cell is a low-power device with low conversion efficiency [10,11], it is essential to incorporate an MPPT algorithm for a PV system. Many algorithms have been developed and investigated for PV systems [12–15]. The power may be extracted from the battery storage system using a charge controller during low solar irradiation and no sunshine hours. A novel battery charging method to prolong battery life without battery current sensors was incorporated for a standalone PV system. Various MPPT techniques [16] have been compared to a single-stage, grid-connected PV system. This proposed system is well appropriate for standalone (off-Grid) systems with proper design of charge/discharge controller for effective battery storage systems and on-grid interactive mode with grid-connected inverter circuits.

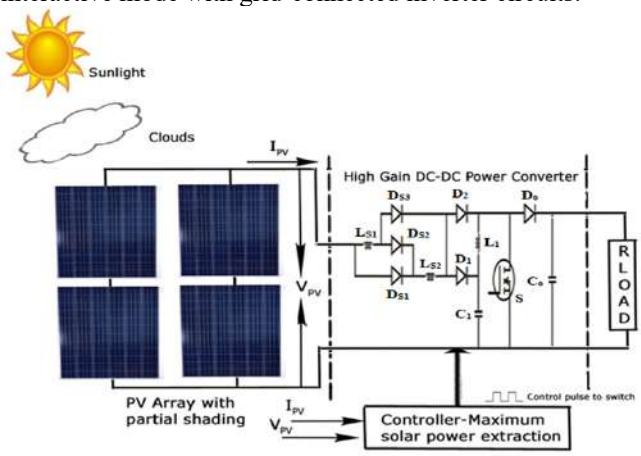

Fig. 1 – Schematic representation of solar PV power generation system with high gain dc-dc converter.

The following is the framework of this research article: Section 2 explores the modeling and simulation of a suggested converter and the experimental investigation of its three operating modes. Section 3 illustrates the modeling and simulation of the PV module and PV characteristic curve under partial shadow conditions. Section 4 explains the implementation of the IIC MPPT algorithm for achieving the extraction of maximum power point (MPP) under different shading conditions of a PV array and compares it with the I&C algorithm. Section 5 deals with implementing an experimental prototype developed in a power electronics laboratory. Section 6 ends with the conclusion part of the research work findings.

2. MODELING AND SIMULATION OF THE PROPOSED CONVERTER

The single switch high gain converter's basic circuit

[1,2]Department of Electrical & Electronics Engineering, Mepco Schlenk Engineering College (Autonomous), Sivakasi, Tamil Nadu, India, Email: trakesh@mepcoeng.ac.in; *sedward@mepcoeng.ac.in.

diagram is proposed and depicted in Fig. 2.

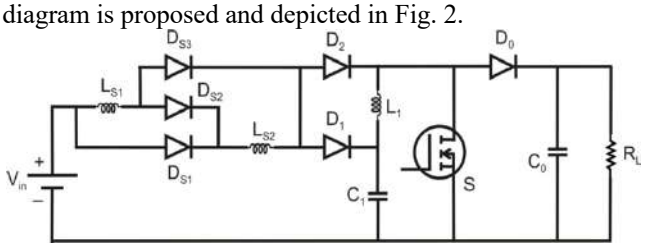

Fig. 2 – Proposed high gain dc-dc converter circuit.

The proposed dc-dc converter has Inductors (L_{s1}, L_{s2}, L_1), a Power switch (S), rectifier diodes (D_{s1}, D_{s2}, D_s, D_1, D_2, and D_0), auxiliary clamping polypropylene or polyester capacitor (C_1), and an output filter electrolytic capacitor (C_0) connected in such a way to give a good voltage profile. The first-order low-pass output circuit comprises a filter capacitor (C_0) and resistance (R_L) to reduce voltage ripples. The structure of the proposed converter is simple and cheaper than the other power converters, which require numerous components.

The following steps were followed to comprehend how the power converter circuit works:

- The forward potential drop across the power switch's resistance is insignificant during the ON state.
- Capacitances have a minimal equivalent series resistance.
- Because the filter capacitance C_0 at the output terminal is usually quite large, each switching cycle can be viewed as an ideal dc voltage.

In Fig. 3, the proposed converter's three modes of operation are depicted under continuous current conduction mode (CCM) during one switching period.

Mode - 1 (t_0–t_1): When S is switched ON:

At time $t = t_0$, D_{s1}, D_{s3}, and D_2 are turned ON, and D_1 and D_2 are OFF, where the inductors (L_{s1} and L_{s2}) are charged from the dc input source, and the energy is transferred to C_0 and the load. The inductor (L_1) is charged at this moment by the stored energy of C_1, which is subsequently released. In the meantime, the energy stored in L_{s1} and, L_{s2} gets released to the clamping capacitance (C_1), and the energy stored in L_1 is released to the filter capacitor (C_0). Thus, i_{Ds1}, i_{Ds3}, and i_{D2} decreased and attained zero at time $t = t_1$, and this mode ends when S is turned OFF.

Mode - 2 (t_1–t_2): When S is switched OFF:

At time $t = t_1$, D_{s2}, D_1, and D_0 are turned ON, and D_{s1}, D_{s3}, and D_2 are turned OFF. Stored energy in L_{s1} and L_{s2} during Mode-1operation starts to discharge, charging the capacitor C_1. Moreover, the energy stored in L_1 is also released to charge C_0 through D_0, which supplies energy to the load. This mode ends at time $t = t_2$ when i_{C1} reaches a constant value.

Mode - 3 (t_2–t_3): When S is switched OFF:

At time $t = t_2$, D_{s2} and D_1 are turned ON, and D_{s1}, D_{s3}, D_0, and D_2 are turned OFF, where the energies of the input voltage source stored in L_{s1} and L_{s2} are released to the clamping capacitor. The output capacitor C_0 delivers energy to the load as the capacitor voltage C_1 increases linearly.

The proposed converter has been compared with the other converters with HF transformer in terms of efficiency, which is shown in Table 1. As demonstrated in Table 1, the recommended power converter appears to have the

The voltage across the switch increases linearly, and this mode ends at time $t = t_3$ when i_{C1} reaches zero. During CCM operation, using volt–second balance on inductors L_{s1}, L_{s2}, and L_1, the following equations are obtained:

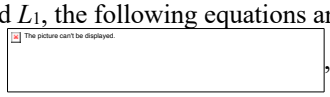

, (1)

. (2)

From eqs. (1) and (2), the steady-state voltage gain of the proposed converter is expressed as below:

Voltage gain = 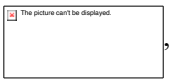

, (3)

where V_{in} – input voltage, V_o – average output voltage, and D-duty cycle

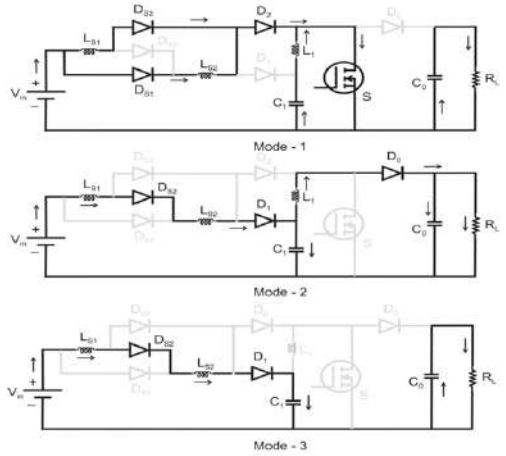

Fig. 3 – Three modes of operation under CCM.

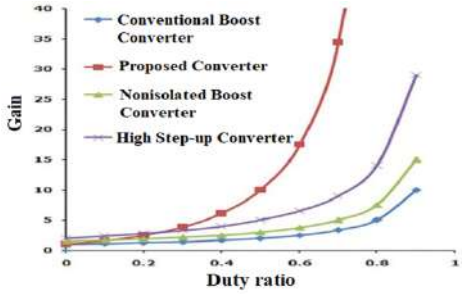

(a)

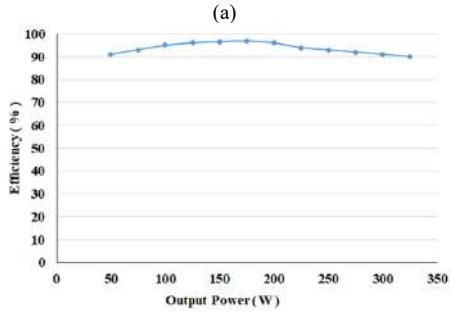

(b)

Fig. 4 – Performance characteristics: (a) Steady-state voltage gain of various converters at varying duty ratio; (b) Efficiency curve of proposed converter for variable output power.

maximum efficiency.

Table 1

Comparison of proposed power converter's efficiency against that of other converters.

References	[8]	[17]	[18]	Proposed
No. of capacitors	5	4	4	2
No. of diodes	7	5	5	6
No. of main switches	2	1	2	1
Coupled inductor/ HF transformer	Yes	Yes	Yes	No
Voltage gain				
Efficiency	93.5 %	92.5 %	94 %	96.68%

Figure 4 shows the steady-state voltage gain and efficiency characteristics of the proposed converter. From Fig. 4(a) it is observed that the proposed converter topology gives high gain than the conventional boost, non-isolated boost, and high step-up converters for the same duty cycle. Figure 5 depicts the suggested power converter's simulated results.

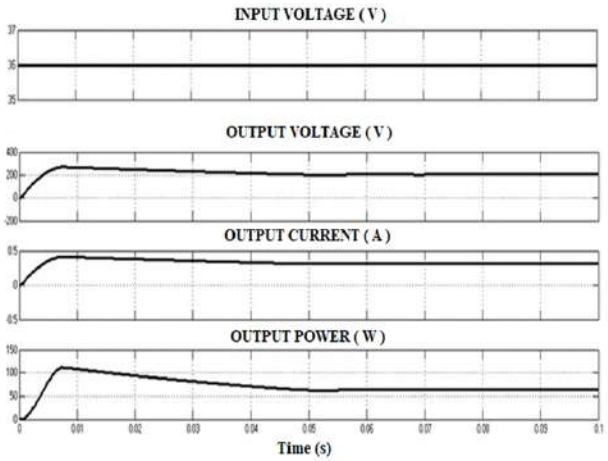

Fig. 5 - Simulation response of input and output waveforms of the converter.

3. MODELING AND SIMULATION OF PV MODULE

The PV module modeling is comprehensively illustrated in an earlier study [19] with the effects of bypass diodes and blocking diodes. Figure 6 depicts a simplified equivalent circuit of a single diode with the influence of series resistance (R_s) and shunt resistance (R_{SH}) in PV cells. The parameters of the PV module have been referred to from the manufacturer datasheet (MS24250) for this analysis purpose.

From the equivalent circuit, the current (I) generated by the PV cell is given by,

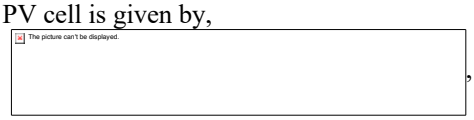

, (4)

where, I_{PH} – generated PV current; I_o – saturation current; V_t – thermal voltage; a – ideal factor value ranges between 1 and 2; V – load voltage.

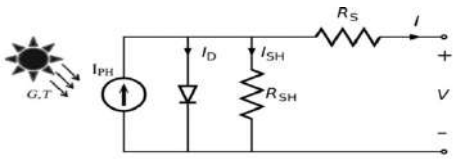

Fig. 6 – Equivalent circuit of a practical PV cell.

A PV array system (2 series & 2 parallel connected PV modules) with bypass diodes and blocking diodes using MATLAB-Simulink under standard test condition (STC: solar irradiation G = 1000 W/m^2 and temperature T = 25 ˚C) are illustrated in Fig. 7. The performance of the PV array under partial shading conditions with two different shading patterns (Table 2) is analyzed, and the simulation responses have been plotted in Fig. 8, where the multiple steps in current-voltage (I-V) curve & multiple peaks in power-voltage (P-V) curve were noticed.

Table 2

PV Array under partial shading conditions.

PV array shading pattern	Operating conditions
Pattern – I	1000 W/m^2, 25°C 800 W/m^2, 25°C
Pattern – II	1000 W/m^2, 25°C 600 W/m^2, 25°C

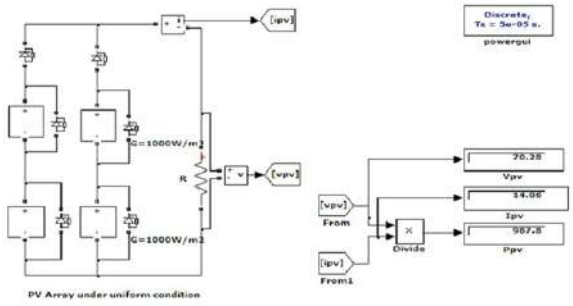

Fig. 7 - MATLAB-Simulink model of PV array under STC.

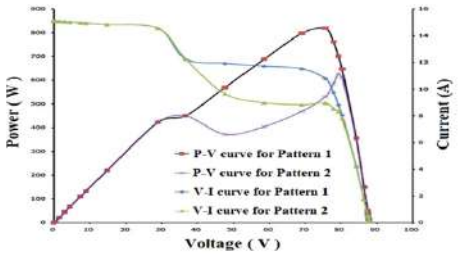

Fig. 8 – I-V and P-V characteristics of PV array under partially shaded conditions.

4. MPPT CONTROL TECHNIQUES

Due to the non-linear behavior of the PV characteristic curve, cost of PV cell, low power, and poor conversion efficiency of photovoltaic module, the importance of the MPPT algorithm to track maximum power to load is discussed. This work compares the performance of incremental conductance (I&C) and improved incremental conductance (IIC) MPPT algorithm for extraction of maximum power under partial shading conditions of the PV array system. The incremental conductance is compared to the instantaneous conductance, and the duty cycle is modified as necessary. In the I&C approach, when the incremental conductance ($\Delta I/\Delta V$) and the array

conductance (I/V) are the same, it transfers the maximum power and locates the maximum voltage (V_{mp}) point, and the controller sustains it until the irradiation changes. Moreover, the incremental conductance of the PV array is exploited to analyze the significant change in (dP/dV).

Even this method provides sufficiently accurate MPP but fails to locate MPP during shading of PV modules in the same string of the PV array, and it assumes a single MPP on the P-V curve. The IC algorithm is perhaps more sophisticated and reliable. With the adoption of IIC, this problem is considerably alleviated. The IIC approach divides the PV operating area into three regions based upon open-circuit voltage (V_{oc}) predicted from the manufacturer datasheet. Area-1 refers from 0 to 70 % of Voc, Area-2 is from 70 % to 80 % of Voc, and Area-3 is from 80 % to Voc, but the MPP location is expected in Area 2, and the reference value is fixed between (70-80) % of Voc to implement the IIC algorithm. The prior knowledge of V_{ref} makes the IIC implementation easier and, with a small increment, helps reduce the tracking time for finding the optimum operating point.

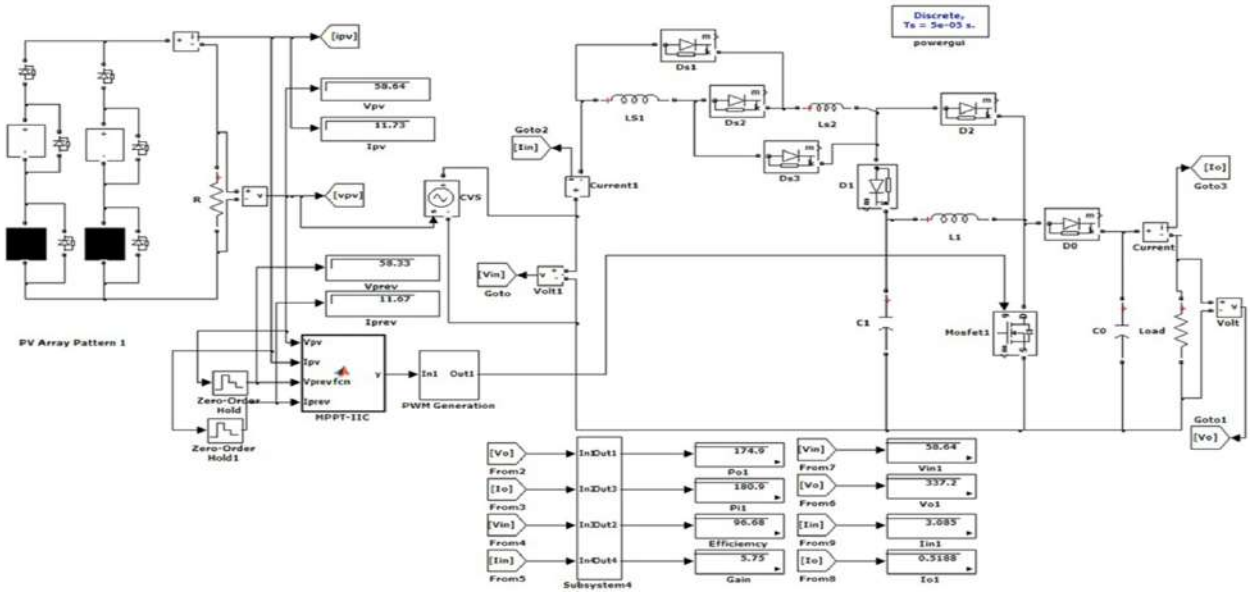

Fig. 9 – MATLAB-Simulink model of a PV array under Pattern-I interfaced with the proposed converter with the IIC algorithm.

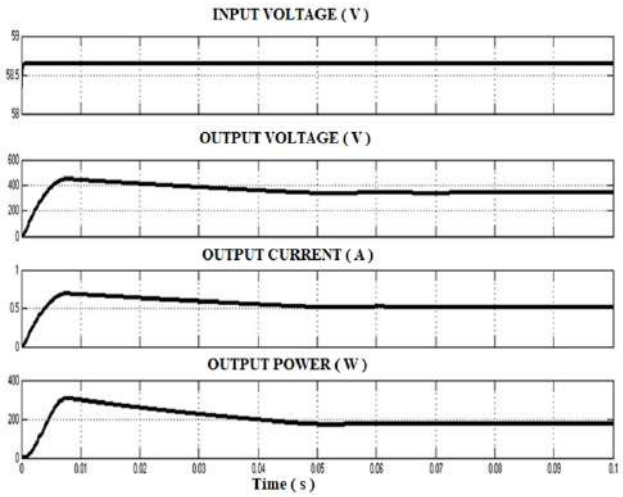

Fig. 10 – Simulation response of proposed PV system.

Table 2 shows that the proposed method tracks the maximum value of power with less power loss, implying that the system's efficiency has increased. In the IIC method, maximum power is tracked effectively compared to the conventional I&C MPPT algorithm by adequately adjusting the duty ratio. The MATLAB-Simulink model and simulation response of the PV array integrated with the dc-dc power converter circuit through the IIC algorithm are illustrated in Fig. 9 and Fig. 10. Table 3 summarises the comparison of the I&C and IIC algorithms for MPPT of PV arrays under partial shading situations.

Table 3
Comparative analysis of I&C and IIC MPPT algorithm under partial shading conditions.

Shading on PV panel	**Pattern - I**		**Pattern - II**	
MPPT controller	**I&C**	**IIC**	**I&C**	**IIC**
V_{IN} (V)	58.64		44.94	
I_{IN} (A)	3.02	3.085	2.294	2.343
P_{IN} (W)	177.1	180.9	103.1	105.3
V_0 (V)	337.3	337.2	256.1	256
I_0 (A)	0.5034	0.5188	0.3822	0.3939
P_0 (W)	169.8	174.9	97.88	100.8
η (%)	95.86	96.68	94.94	95.76

5. A LABORATORY PROTOTYPE

Figure 11 shows the prototype of the proposed high gain dc-dc converter that was implemented for a 10 kHz switching frequency. The specifications are as below: *n*-type MOSFET (IRF840) switch, Inductors ($L_{s1} = L_1 = 1$ mH, $L_{s2} = 0.5$ mH) ferrite core type, capacitors ($C_0 = C_1 = 220$ µF), power diodes (1N5408). PIC (PIC16F877A) generates the pulse width modulation (PWM) signal for switching the converter and is fed to opto-coupler (IC-MCT2E) circuit and gate drive the converter. The hardware prototype was tested at a given variation in the input voltage, and the switching pulse & output voltage were measured using digital storage oscilloscope (DSO),

illustrated in Fig. 12. The experimental results obtained are more consistent with those reported in the simulation.

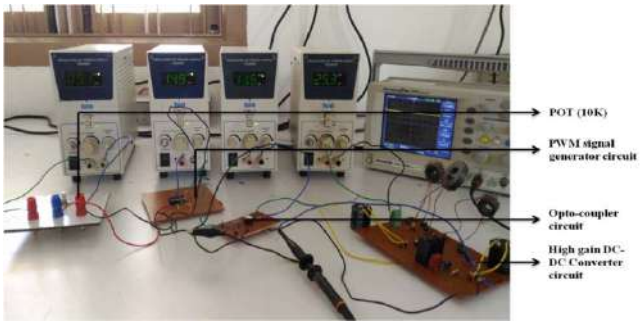

Fig. 11 – Experimental prototype of a proposed dc-dc converter.

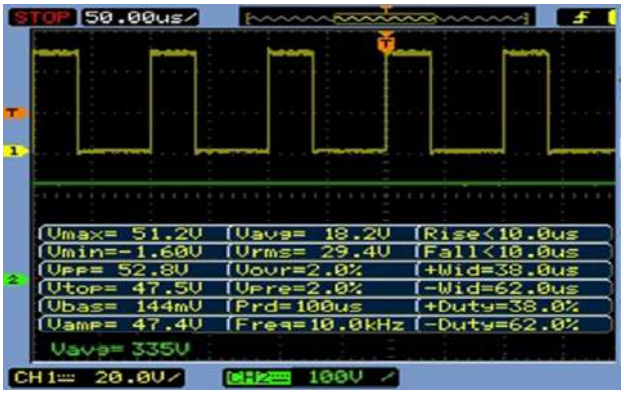

Fig. 12 – Experimental result of gate pulse and output voltage.

Figure 13 shows a laboratory prototype that has been built and experimentally tested for the various input voltage ranges.

Fig. 13 – Experimental prototype of PV interfaced with proposed converter.

Figure 14 shows the voltage across L_{S2} and L_1. The switching pulse (D) and output voltage (V_0) are measured using DSO, and the variation in the duty cycle corresponding to input variation provides constant output voltage, shown in Fig. 15. From Fig. 15, it is noticed that the experimental results are nearer to the simulation results of the proposed system.

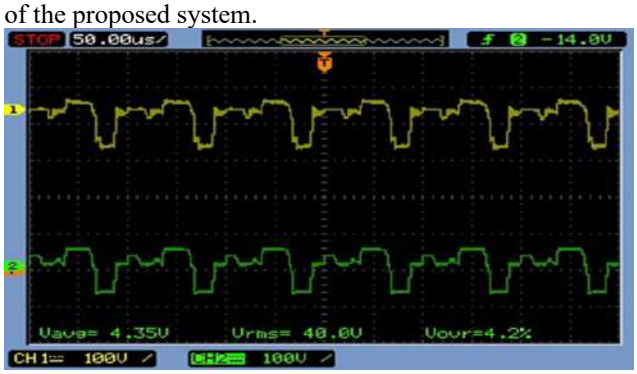

Fig. 14 – Voltage across V_{LS2} and V_{L1}.

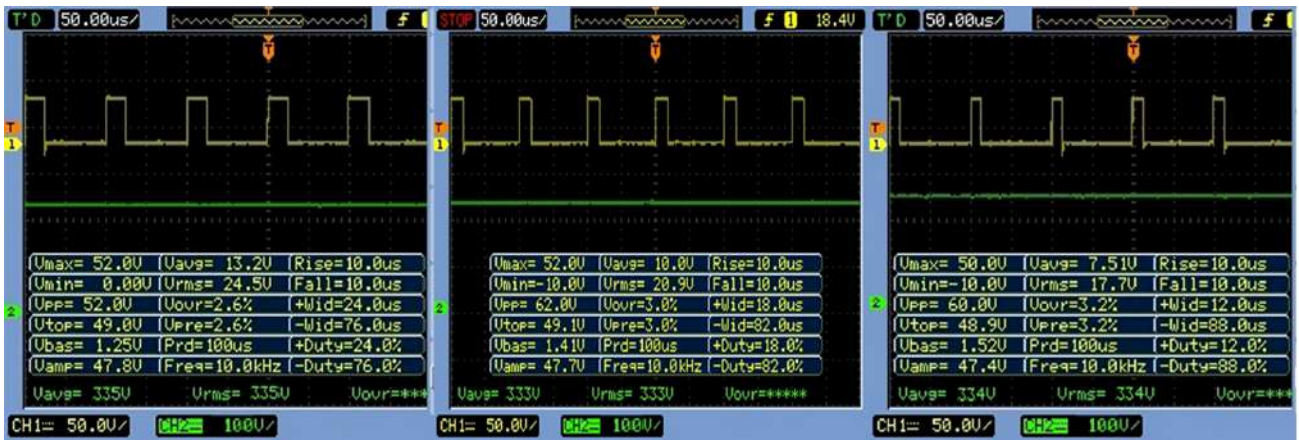

Fig. 15 – Experimental results of D and V_0 under various operating conditions.

6. CONCLUSION

This research paper investigates a novel dc-dc power converter circuit for PV systems under different operating conditions by employing I&C and IIC based MPPT algorithms in a MATLAB-Simulink environment. The comparative study of voltage gain characteristics has been analyzed for different converters with various duty cycle ratios. The recommended converter provides a higher gain ratio for the same duty cycle than a typical boost converter. The simulation responses of the converter are validated through an experimental prototype developed in a power electronics laboratory. Moreover, this converter topology promotes a high gain for PV applications, and it increases the output voltage without using a high-frequency transformer, which reduces the switching losses of the PV system. The MPPT techniques are used to analyse the power converter interfaced PV system, and the results show that the IIC algorithm provides better tracking and extracts a significant amount of solar energy from a PV module than the I&C algorithm under all operating conditions. Moreover, this PV system is well suitable for a standalone (off-Grid) system with proper design of charge controller of battery storage systems and grid-interactive to meet the peak load demands with suitable power inverter circuits.

ACKNOWLEDGEMENTS

The authors would like to express their gratitude to the management and principal of Mepco Schlenk Engineering College (Autonomous), Sivakasi, Tamil Nadu, India, for providing state-of-the-art facilities to conduct our research in collaboration with Anna University in Chennai, Tamil Nadu, India.

Received on 13 July 2021.

REFERENCES

1. C. Huang-Jen, Y. Chun-Jen, L. Yu-Kang, *A dc/dc converter topology for renewable energy systems,* Int. J. Circ. Theor. Appl., **37**, *3*, pp. 485–495 (2009).
2. W. Li, X. He, *Review of non-isolated high-step-up dc-dc converters in photovoltaic grid-connected applications*, IEEE Trans. Ind. Electron., **5**8, *4*, pp. 1239–1250 (2011).
3. F. Tofoli, D. de Souza Oliveira, R. Torrico-Bascope, Y. Alcazar, *Novel nonisolated high-voltage gain dc-dc converters based on 3SSC and VMC*, IEEE Trans. Power Electron., **27**, *9*, pp. 3897–3907 (2012).
4. B. Axelrod, Y. Berkovich, A. Ioinovici, *Switched capacitor/switched-inductor structures for getting transformerless hybrid dc-dc PWM converters*, IEEE Trans. Circuits System, **55**, *2*, pp. 687-696 (2008).
5. C-L. Chen, Y. Wang, J-S. Lai, Y-S. Lee, D. Martin, *Design of parallel inverters for smooth mode transfer microgrid applications*, IEEE Trans. Power Electronics, **25**, *1*, pp. 6–15 (2010).
6. G. Silveira, F. Tofoli, L. Bezerra, R. Torrico-Bascope, *A non-isolated dc-dc boost converter with high voltage gain and balanced output voltage*, IEEE Trans. Ind. Electron., **61**, *12*, pp. 6739–6746 (2014).
7. Z. Guo, D. Sha, X. Liao, J. Luo, *Input-series-output-parallel phase shift full bridge derived dc-dc converters with auxiliary LC networks to achieve wide zero voltage switching range*, IEEE Trans. Power Electron., **29**, *10*, pp. 5081–5086 (2014).
8. J. Javad, *Design of a ZVS PWM dc-dc converter for high gain applications,* Int. J. Circ. Theor. Appl., **44**, *5*, pp. 995-997 (2016).
9. N. Vinh, P. Pierret, A. Michel, S. Chafic, C. Jean-Pierre*, Efficiency of magnetic coupled boost dc-dc converters mainly dedicated to renewable energy systems: influence of the coupling factor,* Int. J. Circ. Theor. Appl., **43**, 8, pp. 1042-1062 (2015).
10. D. Aranzazu, R. Martin Jesus, Vazquez, *Backstepping controller design to track maximum power in photovoltaic systems*, Automatika, **55**, *1*, pp. 22-31 (2014).
11. P. Giovanni, S. Giovanni, V. Massimo, *Distributed maximum power point tracking: challenges and commercial solutions*, Automatika, **53**, *2*, pp. 128-141 (2012).
12. R. Arulmurugan, T. Venkatesan, *Research and Experimental Implementation of a CV-FOINC algorithm using MPPT for PV power* system, Journal of Electrical Engineering Technology, **10**, pp. 1389-1399 (2015).
13. A. Mohammed, Elgendy, Z. Bashar, J. David, Atkinson, *Assessment of perturb and observe MPPT algorithm implementation techniques for PV pumping applications*, IEEE Transactions on Sustainable Energy, **3**, *1*, pp. 21-33 (2012).
14. A. Al-Gizi, A. Craciunescu, M.A. Fadel, M. Louzazni, *A new hybrid algorithm for photovoltaic maximum power point tracking under partial shading conditions*, Rev. Roum. Sci. Techn.– Électrotechn. et Énerg. **63**, *1*, pp. 52–57 (2018).
15. P.S. Sikder, P. Nital, *Incremental conductance-based maximum power point tracking controller using different buck-boost converter for solar photovoltaic system*, Rev. Roum. Sci. Techn.–Électrotechn. et Énerg, **62**, *3*, pp. 269–275 (2017).
16. A. Chitra, S.R.M., Palackal, K. Greeshma, N. Vishwanathan, I. Nambiar, *An incremental conductance-based maximum power point tracking algorithm for a solar photovoltaic system,* International Journal of Applied Engineering Research, **8**, *19*, pp. 2299-2302 (2013).
17. X. Hu, C. Gong, *A high voltage gain DC-DC converter integrating coupled-inductor and diode-capacitor techniques*, IEEE Transactions on Power Electronics, **29**, *2*, pp. 789–800 (2014).
18. T-J. Liang, J-H. Lee, S-M. Chen, J-F. Chen, L-S. Yang, *Novel isolated high-step-up dc–dc converter with voltage lift,* IEEE Transactions on Industrial Electronics, **60**, *4*, pp.1483–1491 (2013).
19. V.M. Gradella, G.J. Rafael, F.E. Ruppert, *Comprehensive approach to modeling and simulation of photovoltaic arrays*, IEEE Transactions on Power Electronics, **24**, *5*, pp. 1198-1208 (2009).